

# Single-Walled Carbon Nanotubes Chemically Functionalized with Polyethylene Glycol Promote Tissue Repair in a Rat Model of Spinal Cord Injury

Jose A. Roman,<sup>1</sup> Tracy L. Niedzielko,<sup>1</sup> Robert C. Haddon,<sup>2</sup> Vladimir Parpura,<sup>3</sup> and Candace L. Floyd<sup>1</sup>

## Abstract

Traumatic spinal cord injury (SCI) induces tissue damage and results in the formation of a cavity that inhibits axonal regrowth. Filling this cavity with a growth-permissive substrate would likely promote regeneration and repair. Single-walled carbon nanotubes functionalized with polyethylene glycol (SWNT-PEG) have been shown to increase the length of selected neurites *in vitro*. We hypothesized that administration of SWNT-PEG after experimental SCI will promote regeneration of axons into the lesion cavity and functional recovery of the hindlimbs. To evaluate this hypothesis, complete transection SCI was induced at the T9 vertebral level in adult female rats. One week after transection, the epicenter of the lesion was injected with 25  $\mu$ L of either vehicle (saline), or 1  $\mu$ g/mL, 10  $\mu$ g/mL, or 100  $\mu$ g/mL of SWNT-PEG. Behavioral analysis was conducted before injury, before treatment, and once every 7 days for 28 days after treatment. At 28 days post-injection the rats were euthanized and spinal cord tissue was extracted. Immunohistochemistry was used to detect the area of the cyst, the extent of the glial scar, and axonal morphology. We found that post-SCI administration of SWNT-PEG decreased lesion volume, increased neurofilament-positive fibers and corticospinal tract fibers in the lesion, and did not increase reactive gliosis. Additionally, post-SCI administration of SWNT-PEG induced a modest improvement in hindlimb locomotor recovery without inducing hyperalgesia. These data suggest that SWNT-PEG may be an effective material to promote axonal repair and regeneration after SCI.

**Key words:** axonal regeneration; gliosis; graft; nanofibers; nanomaterials

## Introduction

**D**ATA from the National Spinal Cord Injury (SCI) Model Systems indicate that a new SCI is sustained approximately every 41 min, with an average of 11,000 new cases each year in the United States. Also, recent estimates suggest that there are over 250,000 persons living with a SCI in the U.S. (National Spinal Cord Injury Statistical Center, 2008). Traumatic SCI causes devastating damage to neurons, axons, and glia, which results in permanent loss of function at and below the injury site. Most SCIs are initiated by rapid displacement of the spinal column, which causes a crushing or contusion of the spinal cord. This initial mechanical impact leads to a secondary injury cascade which involves multiple pathophysiological mechanisms, including excitotoxicity, inflammation, cell death, and axonal loss, and ultimately results in syringomyelia, or the formation of an expanded glial-en-

capsulated cyst (syrinx). While the central cyst is typically surrounded by a rim of spared tissue, the associated spinal cord tissue loss underlies substantial and lasting functional impairment (Anderson and Hall, 1993; Norenberg et al., 2004).

A potentially key element in any approach to regenerate or repair the damaged spinal cord is filling the cyst by administration of a growth permissive/enhancing material. Several biological materials have been used experimentally to promote axon growth across spinal cord lesions, including transplantation of peripheral nerves (Cheng et al., 1996), intact fetal spinal cords or fetal spinal cord tissue (Anderson et al., 1995), Schwann cells (Kuhlengel et al., 1990a, 1990b), stem or progenitor cells of various origins (McDonald et al., 1999; Park et al., 1999), and olfactory-ensheathing glia (Ramon-Cueto et al., 1998). While these studies are intriguing and provide proof of principle for axonal regrowth after SCI, the results show sprouting of only small numbers of axons

<sup>1</sup>Department of Physical Medicine and Rehabilitation, University of Alabama-Birmingham, Birmingham, Alabama.

<sup>2</sup>Departments of Chemistry and Chemical and Environmental Engineering, Center for Nanoscale Science and Engineering, University of California-Riverside, Riverside, California.

<sup>3</sup>Department of Neurobiology, Center for Glial Biology in Medicine, University of Alabama-Birmingham, Birmingham, Alabama.

over a short distance. Additionally, the clinical utility of biological materials such as peripheral nerve explants or stem cells may be limited by lack of reproducible and reliable sources, or even governmental restriction.

As a viable alternative to tissue-derived materials, single-walled carbon nanotubes (SWNTs) have many properties that suggest their potential utility in supporting axonal regeneration and repair after SCI. SWNTs consist of sheets of graphene composed of a single cylinder, 0.4–2.0 nm in diameter. The length can range from one to hundreds of micrometers. Thus, the length and diameter are on a scale similar to that of neuronal processes, suggesting that regenerative substrates made of SWNTs would closely mimic the native CNS tissue topography (Malarkey and Parpura, 2007). SWNTs are electrically conductive, a property that can be manipulated by changing the conformation of carbon atoms in the graphene sheet. Since the charge of the substrate affects axonal growth (Hu et al., 2004), manipulation of their surface charge is an additional beneficial feature. Another feature of SWNTs is that they are strong, durable, and flexible, which are important characteristics for a material implanted into the spinal cord. Carbon nanotubes (CNT) are also not biodegradable, and thus they can exert their potential effects on the injured tissue for a prolonged period of time. Additionally, SWNTs are amenable to modification by attachment of other biomolecules or functionalization (Bekyarov et al., 2005). As used here, functionalization refers to a chemical modification of CNT with a compound. For example, SWNTs adsorb strongly to a wide variety of compounds, including lipids, DNA, peptides, and enzymes, so that in many instances the SWNT needs only to be mixed with the modifying compound (Bekyarov et al., 2005). Modifier compounds can be more permanently attached to SWNTs by covalent linkage (Malarkey and Parpura, 2007). Thus, we hypothesize that SWNTs could be developed and optimized as a material to fill the central cyst and promote axonal regeneration after SCI.

We have previously made various chemically-functionalized CNTs, both SWNTs and multi-walled CNTs (MWNTs), and have demonstrated that these materials promote neuronal growth and neurite outgrowth in cell culture (Hu et al., 2004, 2005; Malarkey et al., 2008, 2009). We also have previously evaluated the neurite-outgrowth-promoting potential of water soluble SWNTs added to the tissue culture media (Ni et al., 2005). To achieve solubility in aqueous solutions, we modified commercially available SWNT-COOH (Carbon Solutions, Riverside, CA) to synthesize SWNT graft co-polymers with either poly-*m*-aminobenzene sulfonic acid (PABS) or polyethylene glycol (PEG). Since the charge of nanotubes can change their neuronal morphological features (Hu et al., 2004), we chose these functionalities so that at physiological extracellular pH of ~7.4, SWNT-PABS and SWNT-PEG would be net-uncharged, either zwitterionic and neutral, respectively. To determine the effects of SWNT-PEG on neurite outgrowth, hippocampal neurons were plated on polyethylene imine (PEI)-coated cover-slips. We found that 1  $\mu\text{g}/\text{mL}$  of SWNT-PEG caused a decrease in the number of neurites per neuron, with a simultaneous increase in the average length of the neurites, which indicates that neurons treated with SWNT-PEG have longer, but sparser, neurites (Hu et al., 2004; Ni et al., 2005). Our previous data suggest that the functionalization of SWNTs is a useful tool to create growth-promoting nanomaterials that could be used for CNS regeneration and repair after

SCI. Specifically, we hypothesize in the current study that post-SCI administration of SWNTs chemically functionalized with PEG will promote tissue repair, axonal regrowth, and functional recovery in a rat model of SCI. Consequently, the goal of the present study was to evaluate this possibility by administering SWNT-PEG (25 or 50  $\mu\text{L}$  of 1, 10, or 100  $\mu\text{g}/\text{mL}$ ), either immediately after or at 1 week post-SCI, using a mid-thoracic transection model with subsequent evaluation of hindlimb locomotion, lesion volume, and markers of gliosis and axonal regeneration or regrowth.

## Methods

### *Experimental groups and spinal cord injury*

All surgical protocols were approved by the Institutional Animal Care and Use Committee of the University of Alabama at Birmingham. Fifty-eight adult female Sprague-Dawley rats (250–300 g, 2 months old) received a complete transection SCI induced by severing the spinal cord at the T9 vertebral level with a MicroFeather ophthalmic scalpel (Feather Safety Razor Co., Osaka, Japan). For the acute administration (5 min after SCI) experiment, the animals were randomly assigned to the following experimental groups: (1) uninjured controls receiving only laminectomy ( $n=6$ ), (2) complete transection SCI ( $n=8$ ), (3) complete transection SCI with post-SCI administration of 10  $\mu\text{g}/\text{mL}$  of SWNT-PEG in a volume of 25  $\mu\text{L}$  ( $n=5$ ), or (4) complete transection SCI with post-SCI administration of 10  $\mu\text{g}/\text{mL}$  of SWNT-PEG in a volume of 50  $\mu\text{L}$  ( $n=5$ ). For the delayed administration experiment, the animals received a treatment 1 week following injury with 25  $\mu\text{L}$  of either vehicle (saline,  $n=8$ ), 1  $\mu\text{g}/\text{mL}$  ( $n=8$ ), 10  $\mu\text{g}/\text{mL}$  ( $n=9$ ), or 100  $\mu\text{g}/\text{mL}$  ( $n=9$ ) of the SWNT-PEG solution stereotaxically injected into the lesion site epicenter. This concentration range was selected based on our previous work evaluating the neurite growth-promoting properties of SWNT-PEG *in vitro* (Ni et al., 2005). For all experiments, MatriStem<sup>®</sup> tissue sealant (Vet; ACell, Inc., Columbia, MD) was placed over the transected dura after administration of SWNTs to seal the dura and prevent overflow of vehicle or SWNT-containing solution into surrounding tissue.

Postoperative animal care was conducted twice daily. Animals received isotonic saline (5 mL SC BID), enrofloxacin (5 mg/kg SC QD), and carprofen (1 mg/kg SC BID) for 7 days post-SCI. Urinary bladders of paraplegic rats were emptied via gentle abdominal compression twice each day for the duration of the experiment. The animals had access to food and water *ad libitum*, including chow placed on the cage floor. The animals were weighed each day and body weight (in grams) was tracked as an indicator of overall health.

### *Anterograde labeling of the corticospinal tract*

Due to the stressful effects of multiple surgeries on the animals, the anterograde labeling of the corticospinal tract was performed 3 days prior to the SCI. Since the axonal transport rate of the tracer is approximately 2–6 mm/d (Reiner et al., 2000; Raju and Smith, 2006), no axons in the thoracic spinal cord would be labeled prior to transection. Additionally, the intensity of tracer labeling has been shown to diminish by 6–7 weeks post-injection (Wouterlood et al., 1990; Raju and Smith, 2006), so labeling 3 days prior to SCI facilitated the evaluation of tracer in spinal cord tissue extracted 5

weeks post-SCI. For this procedure, the animals were anesthetized with inhaled isoflurane (4% induction and 2% maintenance), and four small burr-hole craniectomies were placed 2 mm lateral to the midline, and at anterior-posterior (A/P) coordinates of bregma +1.56 mm and bregma +0.6 mm, such that two each were centered over the right and left motor cortices. Mini-ruby BDA (20  $\mu$ L, 0.1 mg/mL dextran tetramethylrhodamine and biotin in sterile water, Invitrogen/Molecular Probes D-3312; Invitrogen, Carlsbad, CA) was injected stereotaxically into the motor cortex using a 25- $\mu$ L Hamilton syringe and 30-gauge needle (Hamilton Co., Reno, NV), at a rate of 4  $\mu$ L per minute at two depths (dorsal/ventral coordinates -1.5 mm and -2.5 mm).

#### *Behavioral outcome measures*

Locomotor and sensory function was assessed weekly after the injection of the SWNTs (post-SCI days 14–35) using the Basso-Beattie-Bresnahan (BBB) open-field locomotor test, Noldus CatWalk™ gait analysis (Noldus Information Technology, Leesburg, VA), sensitivity to von Frey filaments, and tail-flick analysis.

Hindlimb function was assessed with the BBB locomotor test (Basso et al., 1995) pre-injury, and once each week for the following 35 days. The BBB scale is used to rate gross hindlimb locomotor recovery and ranges from 0 (no hindlimb movement) to 21 (no impairment in walking or gait). For this test, the animals were placed in a 1.2-m-diameter metal, smooth-surfaced activity chamber for 4 min, and hindlimb movement was scored by two investigators who were blinded to the treatment of the animal. All discrepancies in scores were resolved by discussion between the raters at the conclusion of the test and scored to the deficit. Scores were generated for each hindlimb and averaged.

Kinematic analysis was evaluated using the CatWalk gait analysis system (Noldus Information Technology, Leesburg, VA), as previously described (Hamers et al., 2006). In this gait analysis, the animals traverse a glass walkway and a 60-Hz camera digitally records the pawprints. The gait is then analyzed frame by frame with the assistance of integrated software (CatWalk 7.1). One week preceding the injury, the animals were introduced to the procedure and baseline gait parameters were obtained 1 day pre-injury. Subsequent analysis was conducted once every week following the SCI for 35 days.

Mechanical allodynia (hypersensitivity to an originally non-noxious stimulus) was measured by determining the hindpaw withdrawal threshold evoked by stimulation with a series of calibrated von Frey filaments (Stoelting, Inc., Wood Dale, IL). After application of a stimulus of 2 g, 4 g, 6 g, 8 g, 15 g, 26 g, or 60 g to the plantar surface of the hindpaw while the animal stood on a wire grid, the lowest filament receiving at least a 50% positive response of five trials (at least three positive responses) was recorded as the conclusive sensitivity level using the up-down method as previously described (Chaplan et al., 1994). Only animals with plantar placement were evaluated.

Thermal hyperalgesia (heightened response to a noxious stimulus) was evaluated using the tail-flick test as previously described (Deakin and Dostrovsky, 1978). Briefly, a thermal stimulus was elicited by the radiant heat source of a tail-flick unit (Columbia Instruments, Columbus, OH), and was focused on the rat's tail 3–5 cm from the tip. Tail-flick latency

was measured in seconds by a timer connected to a photoelectric cell that upon movement of the tail stopped the timer and heat. Two trials were obtained in each weekly evaluation session and latencies were averaged.

#### *Histological outcome measures*

**Spinal cord tissue preparation.** At 35 days post-SCI, the animals were euthanized with an overdose of pentobarbital (Fatal Plus; Vortech Pharmaceuticals, Dearborn, MI), and perfused with 4% paraformaldehyde (PFA). The spinal cord tissue (1 cm) at the lesion epicenter was extracted, post-fixed for 24 h at 4°C in 4% PFA, and then cryoprotected in increasing concentrations of sucrose (10–30%) for 48 h at 4°C. The spinal cords were then frozen over dry ice, and then blocked into 5-mm longitudinal sections (2.5 mm rostral and caudal from the epicenter). Tissue was then embedded in optimal cutting temperature (OCT) compound (Tissue-Tek™; Fisher Scientific, Pittsburg, PA) and stored at -80°C. Serial longitudinal sections (30  $\mu$ m) were sliced on a cryostat (Leica Microsystems, Inc., Bannockburn, IL), such that the entire spinal cord was sectioned from left to right. Tissue sections were serially placed on 1% gelatin-coated slides and stored at -20°C until further analysis.

**Glial fibrillary acidic protein (GFAP) immunohistochemistry.** A subset of every fifth tissue section was used for GFAP immunohistochemistry. The sections were encircled with a hydrophobic barrier (ImmEdge™; Vector Laboratories, Burlingame, CA), and then dried overnight at room temperature. The slides were processed through graded ascending percentages of alcohol, and blocked with 0.5% H<sub>2</sub>O<sub>2</sub>. The sections were then washed and non-specific reactivity was blocked with 3% goat serum +0.3% Triton X +3% bovine serum albumin +0.1 M phosphate-buffered saline (PBS) at 37°C for 1 h. The tissue sections were rinsed and then incubated in rabbit polyclonal anti-GFAP antibody (1:4000, Z0334; Dako, Carpinteria, CA) for 25 h at 4°C. Afterward, the sections were washed in PBS and incubated in Alexa Fluor® 488 goat anti-rabbit secondary antibody (1:4000, A-11008; Invitrogen) at 4°C for 24 h. The sections were then rinsed, dried overnight, and cover-slipped with Permount mounting medium (Fischer Scientific).

**Neurofilament immunohistochemistry.** Adjacent serial sections (every fifth section) to those utilized for GFAP staining were used for neurofilament immunohistochemistry. The general procedure outlined above for GFAP staining was used for the section preparation, blocking, and tissue/cell permeabilization. The tissue sections were then rinsed and incubated in mouse monoclonal antibody against the 200-kD neurofilament heavy subunit (1:1000, ab24572; Abcam, Cambridge, MA) for 25 h at 4°C. Afterwards, the sections were washed in PBS and incubated in Alexa Fluor 488 goat anti-mouse secondary antibody (1:4000, A-11001; Invitrogen) at 4°C for 24 h. The sections were then rinsed, dried overnight, and cover-slipped with Permount mounting medium.

**Cresyl violet histochemistry.** Adjacent serial sections (every fifth section) to those used for neurofilament staining were processed for histochemistry using cresyl violet acetate (Sigma-Aldrich, St. Louis, MO) as previously described (Kachadroka et al., 2010). Briefly, slide-affixed tissue sections

were dehydrated through ascending ethanol concentrations (70–100%), cleared with xylene, rehydrated in descending concentrations of ethanol (100–70%), and stained in 0.1% cresyl violet acetate (Sigma-Aldrich) for 5 min. The tissue was rinsed in double distilled water (ddH<sub>2</sub>O), and differentiated in 95% ethanol with acetic acid for 2 min, dehydrated with alcohol, washed in xylene, and cover-slipped with Permount.

### Stereological quantification

**Microscopy.** All microscopy was conducted on an Olympus BX51 microscope (Olympus Microscopy, Center Valley, PA) equipped with a motorized stage, and Stereo-Investigator analytical software (MicroBrightField Inc., Colchester, VT). All micrographs were captured as digital images (12-bit color) using a MicroFire 1600×1200-pixel progressive scan interline CCD camera (Optronics, Inc., Goleta, CA).

**Quantification of GFAP immunoreactivity.** GFAP immunoreactivity was measured by calculating the fluorescence intensity in a 50×50- $\mu$ m sampling box. Three non-overlapping sampling boxes were randomly placed in regions of interest at the epicenter, and in regions rostral and caudal to the epicenter such that the medial-most edge of the sampling box was at least 2 mm from the epicenter. Fluorescence intensity (in intensity units) was imaged using a 4× or 10× objective. All intensity values shown in the figures represent raw data, with their pixel intensities within the camera's dynamic range (0–4095) without pixel saturation. All imaging parameters including gain, offset, and exposure time, were set such that intensity values fell within the middle of the dynamic range to avoid pixel saturation. All images were captured with identical settings. Three intensity values per region were averaged. Collecting of images and placement of the sampling boxes for analysis of fluorescence intensity was conducted by a single investigator who was blinded to treatment group.

**Quantification of neurofilament immunoreactivity.** Numbers of neurofilament-positive (NF+) fibers were quantified with unbiased stereology using an optical fractionator probe as previously described (West et al., 1991). Briefly, the epicenter of the lesion was bisected into two regions of interest (ROIs). The rostral-epicenter ROI was comprised of tissue from the left half of the epicenter of the lesion to 500  $\mu$ m rostral to the epicenter. Similarly, the epicenter-caudal ROI included tissue from the right half of the lesion epicenter to 500  $\mu$ m caudal to the lesion. NF+ fibers were counted using the optical fractionator probe with a 20× objective in every fifth serial section. Inclusion criteria were set such that only NF+ fibers with a minimum length of 5  $\mu$ m were counted. Outlining of the serial sections and counting was conducted by a single investigator blinded to treatment group. The total approximation by the optical fractionator and the second coefficient of error were calculated, and a value of 0.1 for the second coefficient of error was accepted.

**Quantification of lesion volume.** Lesion volume was assessed in tissue sections processed for cresyl violet histochemistry, and was quantified based using the Cavalieri estimator. Briefly, the border of intact and damaged tissue was delineated by an investigator blinded to treatment group using a 10–20× objective, and the lesion area of each section

was obtained. Cystic cavities were included in the analysis as lesion tissue (see black arrows in Fig. 2). The Cavalieri probe was then used to estimate total lesion volume.

**Corticospinal tract (CST) axonal counting.** A single investigator who was blinded to treatment group quantified BDA-positive axons. In order to quantify these axons, a line was drawn across the spinal cord transversely 500  $\mu$ m rostral from the lesion epicenter, and BDA-labeled axons intersecting this line were counted in every fifth serial section throughout the spinal cord.

### Functionalization of SWNT

We used commercially-available, purified P3-SWNT with carboxylic acid groups at their ends (SWNT-COOH; Carbon Solutions) that were functionalized as we previously described (Ni et al., 2005; Malarkey et al., 2008). Briefly, the acyl chloride intermediate product SWNT-COCl was generated by adding oxalyl chloride drop by drop to the dispersion of SWNT-COOH. After removal of oxalyl chloride excess, SWNT-COCl were functionalized with polyethylene glycol (PEG) to form the graft copolymer. Following removal of PABS excess, the final product SWNT-PEG was collected on the membrane, dried under a vacuum overnight, and then reconstituted in ddH<sub>2</sub>O, yielding a 5-mg/mL stock solution. This stock solution was diluted in the normal external (vehicle) saline composed of (in mM): NaCl (140), KCl (5), CaCl<sub>2</sub> (2), MgCl<sub>2</sub> (2), glucose (5), and HEPES (10) (pH = 7.4).

### Statistical analysis

Data are shown as mean  $\pm$  standard error of the mean (SEM), and were analyzed using SigmaPlot<sup>®</sup> (v11; Systat Software Inc., San Jose, CA). Data were analyzed using one-way analysis of variance (ANOVA), or a repeated-measures ANOVA, followed by the Holm-Sidak *post-hoc* analysis for all pair-wise multiple comparisons. Pearson product moment calculations were conducted using SigmaStat. Statistical significance was set at  $p < 0.05$ .

## Results

### Acute post-SCI administration of SWNT-PEG promotes tissue repair and does not increase reactive gliosis

In the first experiment, we evaluated the effect of acute (5 min) post-SCI administration of SWNT-PEG on axonal morphology using immunohistochemistry of NF+ fibers in serial longitudinal sections of the rat spinal cord at the epicenter. Comparisons were made between uninjured controls receiving only laminectomy (LAM), SCI with no SWNT-PEG, SCI+25  $\mu$ L of SWNT-PEG (10  $\mu$ g/mL), or SCI+50  $\mu$ L of SWNT-PEG (10  $\mu$ g/mL). Stereological quantification (Fig. 1) showed that, as expected, SCI caused a significant decrease in NF+ fibers compared to animals receiving only laminectomy (LAM), but no SCI. Additionally, we found that acute post-SCI administration of 25 or 50  $\mu$ L of 10  $\mu$ g/mL SWNT-PEG induced a significant increase in NF+ fibers compared to non-treated, injured animals (SCI). These data suggest that acute post-SCI treatment with SWNT-PEG promotes axonal survival and repair in tissue surrounding the transection cavity after a spinal cord injury. Since both the 25- and 50- $\mu$ L infusions had similar effects when administered acutely after SCI, the 25- $\mu$ L volume

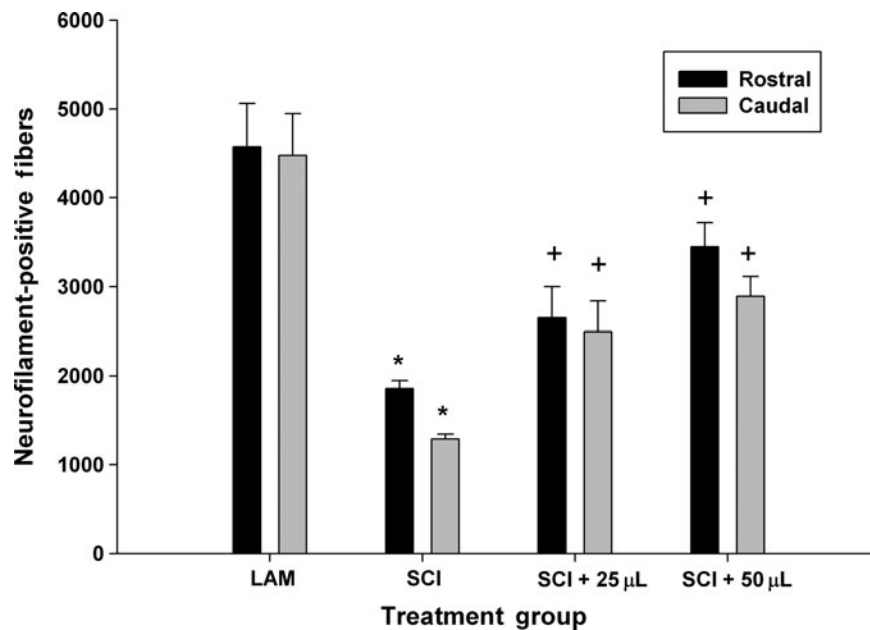


**FIG. 1.** Effect of acute post-SCI administration of SWNT-PEG after SCI. Animals received a complete transection SCI, and immediately following injury either 25 or 50  $\mu\text{L}$  of SWNT-PEG (10  $\mu\text{g}/\text{mL}$ ) was stereotaxically injected into the lesion epicenter. At 35 days post-SCI, tissue was extracted and the numbers of neurofilament-positive (NF+) fibers were counted in regions of interest rostral-epicenter (Rostral) and epicenter-caudal (Caudal). SCI induced a significant reduction in NF+ fibers compared to the uninjured controls (LAM, laminectomy only) group (\*). Both the 25- and 50- $\mu\text{L}$  volumes of SWNT-PEG significantly increased the number of NF+ fibers as compared to the SCI group (+; SCI, spinal cord injury; SWNT-PEG, single-walled carbon nanotubes functionalized with polyethylene glycol).

was used in the subsequent experiments to evaluate the effect of delayed post-SCI administration of SWNT-PEG.

#### *Delayed administration of SWNT-PEG reduces lesion volume in a concentration-dependent manner*

After determining that acute post-SCI administration of SWNT-PEG promoted axonal sparing and/or repair, we evaluated a more clinically-relevant delayed administration at 1 week post-injury. The experimental groups evaluated were SCI+25  $\mu\text{L}$  of either 0, 1, 10, or 100  $\mu\text{g}/\text{mL}$  SWNT-PEG in normal saline. Lesion volume was calculated in longitudinal serial sections at the epicenter in tissue extracted at 35 days post-SCI, and subsequently processed for cresyl violet histochemistry (Fig. 2). As seen in Figure 2A, animals that received delayed post-SCI administration of vehicle (0  $\mu\text{g}/\text{mL}$  SWNT-PEG; sham-treatment) had very large lesion areas. As seen in Figure 2B–D, the lesion area was reduced by post-SCI administration of SWNT-PEG, particularly at higher concentrations. Quantification of the total lesion volume (Fig. 2E) using the Cavalieri estimator showed that post-SCI administration of 100  $\mu\text{g}/\text{mL}$  of SWNT-PEG significantly reduced lesion volume compared to the 0- $\mu\text{g}/\text{mL}$  group. This reduction occurred as an overall decrease in lesion volume, and was visible in both the white and gray matter.

#### *Delayed administration of SWNT-PEG increases the number of neurofilament-positive fibers in the lesion epicenter*

We next sought to determine the effect of delayed administration of SWNT-PEG on the number of NF+ fibers in the

epicenter and adjacent regions as an indicator of regeneration and repair. As shown in Figure 3A, NF+ fibers were visualized in ROIs rostral-epicenter (white box) and epicenter-caudal (yellow box). As expected, we observed many NF+ fibers in spinal cord tissue from control rats that received only laminectomy (Fig. 3B). SCI substantially reduced the number of NF+ fibers observed as compared to uninjured controls (Fig. 3C). Additionally we found that delayed post-SCI administration of SWNT-PEG, in a concentration-dependent manner, increased the number of NF+ fibers observed (Fig. 3D–F). Quantification of the number of NF+ fibers (Fig. 3G) demonstrated that there were significantly fewer NF+ fibers in the SCI+vehicle (0  $\mu\text{g}/\text{mL}$ ) group compared to the uninjured control (LAM) group, in both the rostral-epicenter and epicenter-caudal ROIs. Also, delayed post-SCI administration of 1  $\mu\text{g}/\text{mL}$  of SWNT-PEG did not significantly increase the number of NF+ fibers, although a trend toward an increase was observed. However, the medium (10  $\mu\text{g}/\text{mL}$ ) and high (100  $\mu\text{g}/\text{mL}$ ) concentrations of SWNT-PEG caused a significant increase in NF+ fibers in both the rostral-epicenter and epicenter-caudal regions compared to the vehicle group (0  $\mu\text{g}/\text{mL}$ ). These data indicate that delayed post-SCI administration of SWNT-PEG at the medium and high concentrations increases the numbers of axons present at the lesion epicenter.

#### *Delayed administration of SWNT-PEG promotes modest sprouting of corticospinal tract axons into the lesion epicenter*

Although we found that administration of SWNT-PEG increased NF+ fibers, NF is ubiquitously expressed in spinal cord axons, and therefore is not specific for a particular tract or

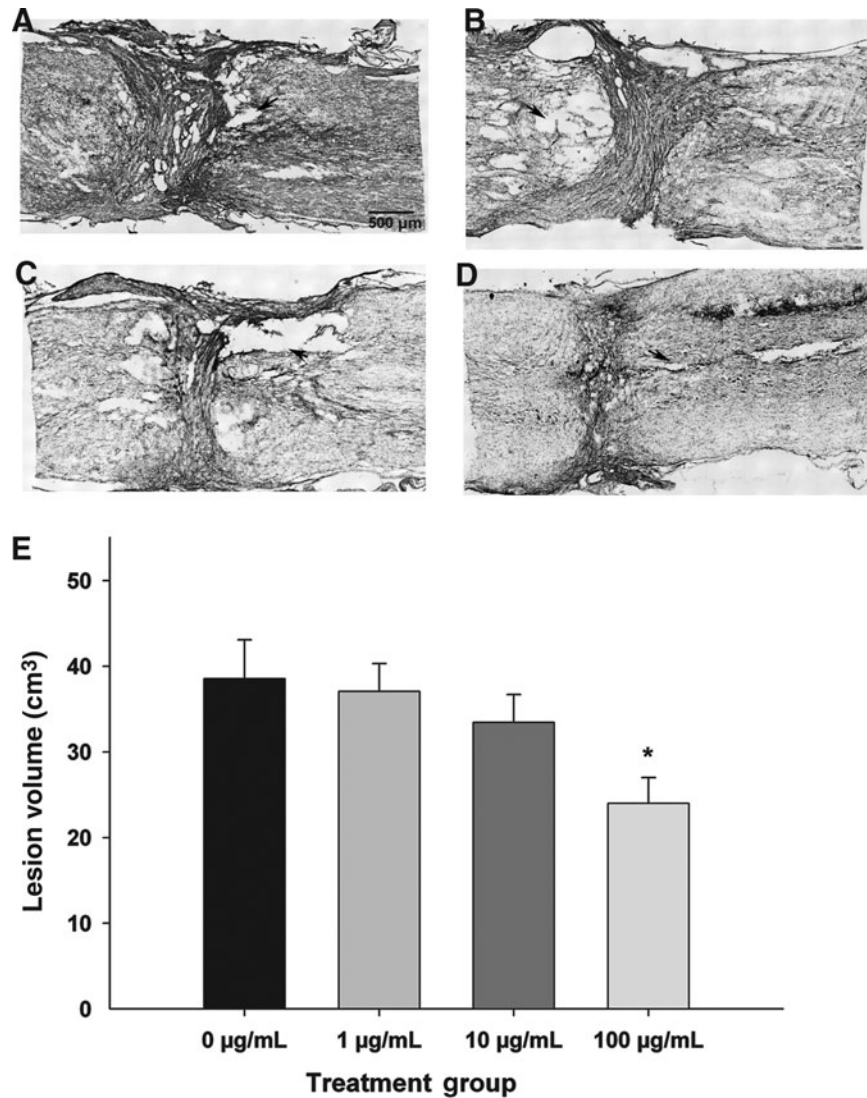


**FIG. 2.** Effect of delayed post-SCI administration of SWNT-PEG on lesion volume. Animals received a complete transection SCI and 7 days later 25  $\mu$ L of SWNT-PEG (0–100  $\mu$ g/mL) was stereotactically injected into the lesion epicenter. Tissue was extracted at 35 days post-SCI and processed using cresyl violet histochemistry to identify the lesion cytoarchitecture. Representative micrographs from animals that received 0  $\mu$ g/mL (A), 1  $\mu$ g/mL (B), 10  $\mu$ g/mL (C), or 100  $\mu$ g/mL (D) of SWNT-PEG are shown. Cystic cavities were included as lesion tissue, and examples are denoted by black arrows (scale bar = 500  $\mu$ m). Total lesion volume was estimated using the Cavalieri estimator in serial sections (E). Delayed post-SCI administration of SWNT-PEG (100  $\mu$ g/mL) caused a statistically significant reduction in lesion volume (indicated by \*; SCI, spinal cord injury; SWNT-PEG, single-walled carbon nanotubes functionalized with polyethylene glycol).

subset of axons. Consequently, we used tract tracing of the corticospinal tract (CST) to evaluate the effects of delayed post-SCI administration of SWNT-PEG on CST axons in the lesion. We quantified the number of labeled CST axons at a site 500  $\mu$ m rostral to the epicenter of the lesion, which corresponds to the edge of the rostral-epicenter ROI used for quantification of NF+ fibers in Figure 3. As seen in Figure 4A, few BDA-labeled CST axons were visualized in this rostral-epicenter region. Quantification of BDA-labeled axons (Fig. 4B) indicated that very few axons were found in animals that received vehicle or 1  $\mu$ g/mL SWNT-PEG 7 days after SCI. Additionally, we found that post-SCI administration of the medium (10  $\mu$ g/mL) or high (100  $\mu$ g/mL) concentration of SWNT-PEG significantly increases the number of BDA-

labeled CST axons in the rostral-epicenter region, although the total number of BDA-labeled axons in all SCI groups was modest. No CST-labeled axons were identified in the epicenter-caudal ROI (data not shown).

*Delayed administration of SWNT-PEG does not alter reactive astrogliosis at the lesion epicenter or in proximal regions*

GFAP immunoreactivity was analyzed to evaluate the effects of delayed post-SCI administration of SWNT-PEG on reactive astrogliosis at the lesion epicenter and in proximal regions in tissue extracted at 35 days post-SCI (Fig. 5A). As seen in Figure 5B–E, little GFAP expression was detected at

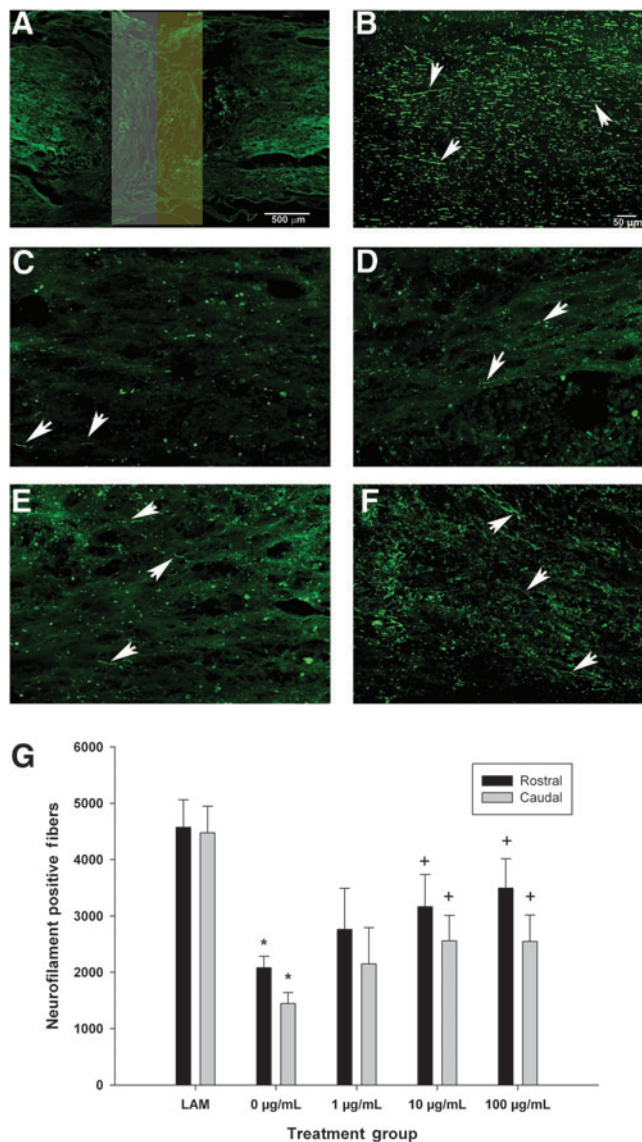


**FIG. 3.** Effect of delayed post-SCI administration of SWNT-PEG on expression of neurofilament in regions of interest (ROIs) at the lesion epicenter. Neurofilament-positive (NF+) fibers were analyzed in two regions of interest, the rostral-epicenter (rostral, white box), and the epicenter-caudal (caudal, yellow box), as shown in panel **A** (scale bar=500 µm). Representative micrographs from an uninjured control animal (LAM, **B**), and animals that received SCI+0 µg/mL (**C**), 1 µg/mL (**D**), 10 µg/mL (**E**), or 100 µg/mL (**F**) are shown. Arrows indicate NF+ fibers (scale bar=50 µm). Stereological quantification of NF+ fibers (**G**) demonstrated that SCI caused a significant decrease in NF+ fibers (\*=statistically significant between the LAM versus the 0-µg/mL SWNT-PEG group). Delayed post-SCI administration of SWNT-PEG caused a significant increase in NF+ fibers in the 10- and 100-µg/mL group compared to the 0-µg/mL group in both the rostral and caudal ROIs (indicated by +; SCI, spinal cord injury; SWNT-PEG, single-walled carbon nanotubes functionalized with polyethylene glycol). Color image is available online at [www.liebertpub.com/neu](http://www.liebertpub.com/neu).

the lesion epicenter, and a marked increase in GFAP-immunoreactivity was detected in regions rostral and caudal to the lesion epicenter, consistent with the production of an astrocyte barrier to encapsulate the lesion. Upon quantification of the GFAP immunoreactivity (Fig. 5F), we found no significant differences between the sham-treated (0 µg/mL SWNT-PEG) group and the SWNT-PEG-treated groups (1–100 µg/mL), which suggests that delayed post-SCI administration of SWNT-PEG did not alter or induce reactive astrogliosis in the lesion epicenter or in adjacent regions rostral or caudal to the epicenter.

#### *Delayed administration of SWNT-PEG promotes modest functional recovery of hindlimb locomotion*

We evaluated the effects of delayed administration of SWNT-PEG on functional recovery of hindlimb locomotion using the Basso-Beattie-Bresnahan (BBB) open field test as previously described (Basso et al., 1995; Chaovipoch et al., 2006; Kachadroka et al., 2010), and kinematic analysis of hindlimb use with the CatWalk gait analysis system (Hamers et al., 2006). Behavioral tests were conducted on post-SCI day 5 (prior to administration of SWNT-PEG), and then once per week for 35 days post-SCI beginning 7 days after the administration of SWNT-PEG, which corresponds to post-SCI day 14. As shown in Figure 6, animals receiving SCI+SWNT-PEG at either 1, 10, or 100 µg/mL showed a trend toward improved BBB scores compared to animals that received SCI+vehicle (0 µg/mL). However, this improvement reached statistical significance only for the highest concentration (100 µg/mL) on post-SCI day 35. Notably, there was a large amount of variability in the BBB scores, and the functional recovery observed was modest. Taken together, these data suggest that there was a trend for delayed post-SCI administration of SWNT-PEG to increase recovery of locomotor function compared to animals that received no treatment.

Figure 7 shows the results of the CatWalk kinematic analysis of hind pawprint area, which indicates the maximal contact area of the plantar surface of the paw in stance, whereby larger print areas indicate more plantar contact. Animals that received the 100-µg/mL treatment showed a trend toward increased maximum pawprint area at day 35 post-injury, but this was not statistically significant. These data suggest that the 100-µg/mL concentration of SWNT-PEG may improve the ability of the animals to plantar-place the hindlimb, an indicator of improved hindlimb locomotor recovery. Other kinematic measures, including regularity index and stride length, were analyzed; however, these measures require consistent plantar placement and completion of at least one full step cycle, and most animals did not regain enough functional recovery to be included in these analyses (data not shown).

#### *Post-SCI administration of SWNT-PEG does not induce neuropathic pain*

Allodynia was evaluated using von Frey filaments. However, similarly to the kinematic measures, this evaluation tool requires consistent plantar placement of the hindpaw, and very few animals were able to be analyzed after SCI, thereby rendering the data inconclusive (data not shown). Figure 8 shows the latency of a response due to a thermal stimulus in the tail-flick assay. After SCI but before administration of SWNTs (post-injury day 5, black bars), the reaction time to the thermal stimulus was decreased compared to the pre-injury

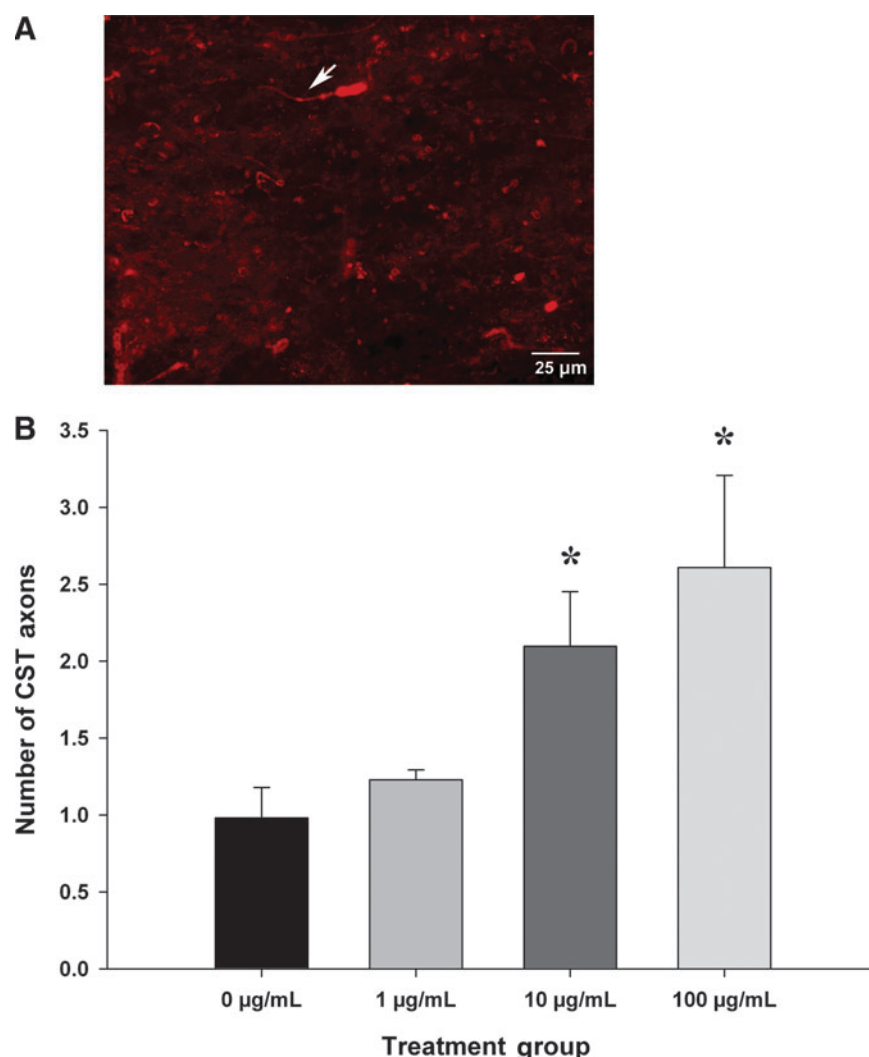


**FIG. 4.** Effect of delayed post-SCI administration of SWNT-PEG on corticospinal tract (CST) axonal growth. Prior to SCI, the CST neurons were labeled with BDA (mini-ruby). Labeled CST axons that were identified in the rostral-epicenter region of interest (ROI) were analyzed. **(A)** Representative micrograph from the 100- $\mu\text{g}/\text{mL}$  SWNT-PEG group, showing a BDA-labeled axon (arrow; scale bar = 25  $\mu\text{m}$ ). **(B)** Quantification of BDA-labeled axons at the edge of the rostral-epicenter ROI (500  $\mu\text{m}$  rostral to the epicenter) showed that delayed administration of 10 and 100  $\mu\text{g}/\text{mL}$  SWNT-PEG induced a significant increase in BDA-labeled CST axons (indicated by \*; SCI, spinal cord injury; SWNT-PEG, single-walled carbon nanotubes functionalized with polyethylene glycol; BDA, dextran tetramethylrhodamine and biotin in sterile water). Color image is available online at [www.liebertpub.com/neu](http://www.liebertpub.com/neu).

values (white bars), indicating that SCI induced alterations in reaction time. However, no significant differences in tail-flick latency were observed between post-injury day 5 values (before administration of SWNT), and post-injury day 14–35 values (after SWNT administration) for any treatment group. Also, no significant differences in latency between post-SCI day 14 and post-SCI days 21–35 were found for any treatment group. These data suggest that delayed post-SCI administration of SWNTs after SCI did not significantly alter pain sensation below the level of the lesion, and that SWNT administration did not induce hyperalgesia.

#### *Delayed post-SCI administration of SWNT-PEG does not induce overt toxicity*

The overall health and well-being of the experimental animals was monitored daily, and the body weight of each ani-

mal was recorded in the morning after manual bladder expression. As seen in Figure 9, the animals lost body weight each day in the first 5 days post-SCI (before SWNT administration), which is likely attributable to the stress induced by the SCI. By post-SCI days 5–6, the body weights of the animals in each treatment group stabilized. No significant differences were found between the average body weights recorded on post-SCI day 5 and post-SCI days 8–35 (after SWNT-PEG administration) for any treatment group evaluated, which suggests that delayed post-SCI administration of SWNT-PEG does not cause a decline in overall health.

#### *Functional outcome measures correlate with histological markers of tissue sparing*

The Pearson product moment correlation coefficient ( $r$ ) was calculated to determine the relationship between the BBB

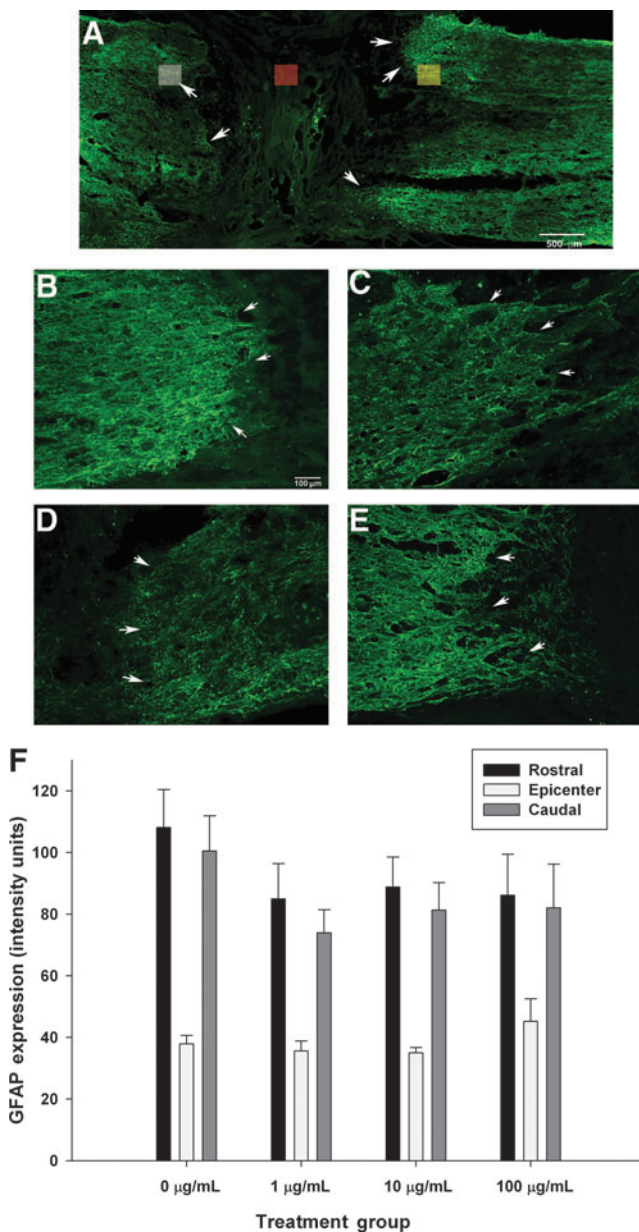


**FIG. 5.** Effect of delayed post-SCI administration of SWNT-PEG on GFAP-immunoreactivity. GFAP-immunoreactivity (GFAP-IR) was measured in regions of interest (ROIs) at the epicenter (red box), rostral (white box) and caudal (yellow box), as shown in panel A. White arrows indicate the border of reactive astrogliosis (scale bar = 500  $\mu\text{m}$ ). Representative micrographs from animals that received SCI + 0  $\mu\text{g}/\text{mL}$  (B), 1  $\mu\text{g}/\text{mL}$  (C), 10  $\mu\text{g}/\text{mL}$  (D), or 100  $\mu\text{g}/\text{mL}$  (E) are shown. Arrows indicate the border of reactive astrogliosis (scale bar = 100  $\mu\text{m}$ ). (F) Fluorescence intensity was quantified (intensity units), and it was found that delayed post-SCI administration of SWNT-PEG did not significantly alter GFAP-IR in any ROI compared to the sham (0  $\mu\text{g}/\text{mL}$ ) treatment group (SCI, spinal cord injury; SWNT-PEG, single-walled carbon nanotubes functionalized with polyethylene glycol; GFAP, glial fibrillary acidic protein). Color image is available online at [www.liebertpub.com/neu](http://www.liebertpub.com/neu).

score on day 35, lesion volume ( $\mu\text{m}^3$ ), and neurofilament-positive fibers rostral and caudal to the injury site. We found that as lesion volume (data from Fig. 2) decreases, BBB scores (data from Fig. 6) increase in a statistically significant relationship ( $r = -0.446$ ;  $p < 0.05$ ). Additionally, we found that as the number of neurofilament-positive fibers caudal to the injury (data from Fig. 3) increases, the BBB score on day 35 increases in a statistically significant relationship as well ( $r = 0.635$ ;  $p < 0.05$ ); such a correlation could not be established when the number of neurofilament-positive fibers rostral to the injury were considered ( $r = 0.0167$ ). These data indicate that recovery of functional outcome was greatest in animals with lower lesion volumes and more axons caudal to the lesion.

## Discussion

In this study we evaluated the central hypothesis that SWNT-PEG, a nanomaterial that has been shown to promote neurite outgrowth *in vitro* (Ni et al., 2005), would promote tissue repair and functional recovery after SCI in a rat model. We report that acute post-SCI administration of SWNT-PEG increased the numbers of neurofilament-positive fibers compared to the injured, non-treated group. Secondly, we evaluated a more clinically-relevant delayed administration time point of 1 week post-SCI. We found that delayed post-SCI administration of SWNT-PEG significantly reduced lesion volume, significantly increased the number of neurofilament-positive fibers and CST fibers in and around the lesion epicenter, and did not induce reactive gliosis or overt toxicity. Additionally, we found that delayed post-SCI administration of SWNT-PEG at 100  $\mu\text{g}/\text{mL}$  induced modest hindlimb functional recovery, which was correlated with histological markers of tissue repair. Importantly, this is the first report to indicate that SWNT-PEG promotes repair and regeneration of damaged CNS tissue *in vivo*.

The research idea of engineering a biocompatible material to promote tissue repair and regeneration after SCI is well-established (Bunge and Pearse, 2003; Novikova et al., 2003; Potter et al., 2008; Tabesh et al., 2009); however, the development of an efficacious substrate for use as scaffolding remains an area of active, ongoing research by many teams. Guidance channels or bioengineered scaffolds (i.e., fibrin or hydrogel) have previously been evaluated in rodent *in vivo* models of SCI with encouraging, albeit incomplete, success (Calancie et al., 2009; Johnson et al., 2010a; Oudega et al., 2001; Potter et al., 2008; Xu et al., 1995). An additional approach is to enhance the scaffold characteristics by the addition of growth-promoting cells, proteins, or drugs. For example, Wang and colleagues developed an injectable hydrogel comprised of hyaluronan and methylcellulose that releases nimodipine as a potential regenerative scaffold (Wang et al., 2009). However, this scaffold has not been evaluated *in vivo*. With regard to *in vivo* studies, fibrin scaffolds modified to release growth factors and seeded with embryonic stem cell-derived neuronal progenitor cells were shown to increase the survival and differentiation of neural progenitor cells following transplantation in a rat model of SCI (Johnson et al., 2010b). Similarly, a hydrogel (based on hyaluronic acid) containing brain-derived neurotrophic factor and seeded with mesenchymal stem cells promoted modest regeneration, repair, and functional recovery in a rat model of SCI (Park et al., 2010).

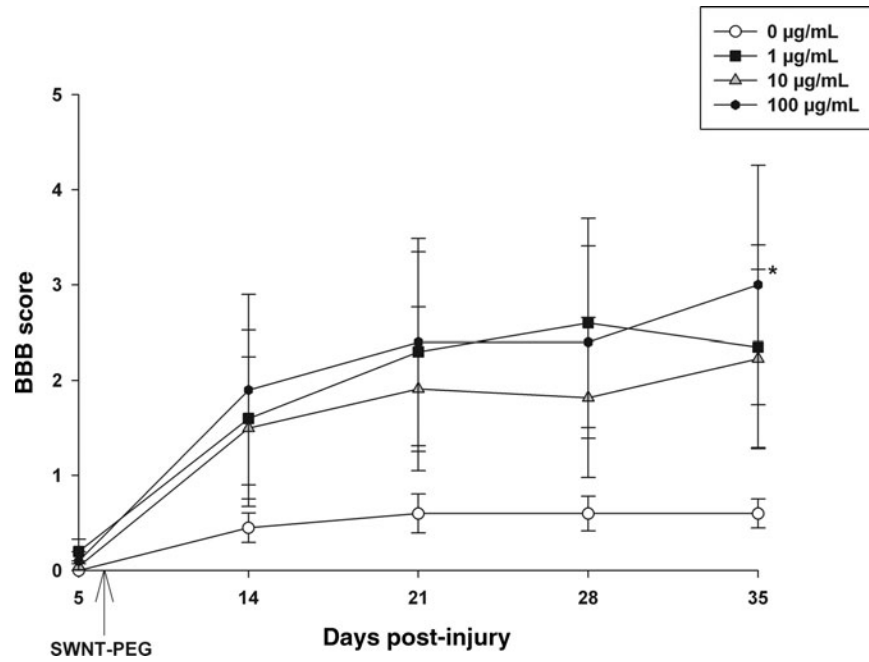


**FIG. 6.** Effect of delayed post-SCI administration of SWNT-PEG on hindlimb locomotor recovery. Hindlimb locomotion was rated in the open field by two evaluators who were blinded to treatment group using the BBB scale. On day 5 post-SCI and prior to administration of SWNT-PEG, the animals showed little to no spontaneous movement of the hindlimbs. Animals that received the SCI+0 µg/mL SWNT-PEG treatment showed very little functional recovery, while post-SCI administration of SWNT-PEG induced improvements in BBB scores, reaching statistical significance on post-SCI day 35 for the 100-µg/mL SWNT-PEG group compared to the 0-µg/mL group (indicated by \*). SWNT-PEG administration time is indicated by the arrow (post-SCI day 7; SCI, spinal cord injury; SWNT-PEG, single-walled carbon nanotubes functionalized with polyethylene glycol; BBB, Basso-Beattie-Bresnahan).

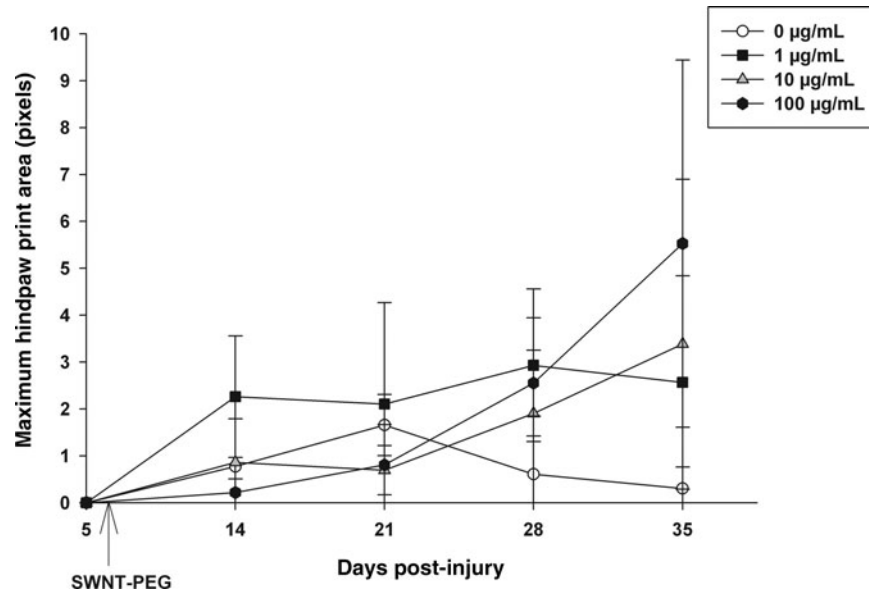


**FIG. 7.** Effect of delayed post-SCI administration of SWNT-PEG on hind pawprint area. Hind pawprint area during overground locomotion was analyzed in the step cycle using the CatWalk kinematic analysis system. On day 5 post-SCI and prior to administration of SWNT-PEG, the animals in all groups did not plantar-place the hindpaws. Animals that received the 0-µg/mL concentration of SWNT-PEG showed very little hindpaw placement, and post-SCI administration of SWNT-PEG induced a trend toward increased hindpaw placement, but this did not reach statistical significance. SWNT-PEG administration is indicated by the arrow (post-SCI day 7; SCI, spinal cord injury; SWNT-PEG, single-walled carbon nanotubes functionalized with polyethylene glycol).

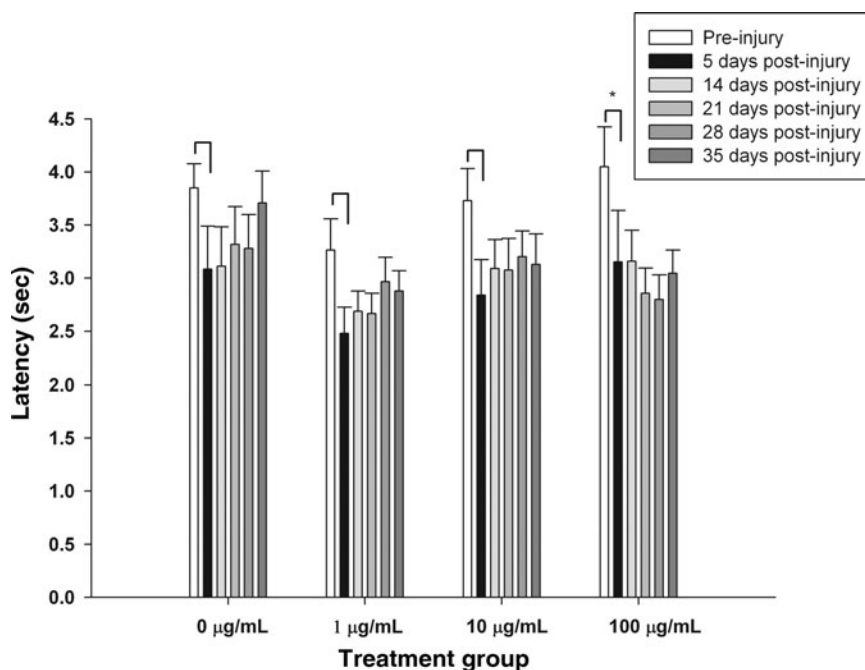


**FIG. 8.** Effect of delayed post-SCI administration of SWNT-PEG on tail-flick latencies. Response latency (in seconds) to a thermal stimulus applied to the tail was evaluated prior to SCI (white bars), after SCI but prior to treatment (black bars, 5 days post-injury), and at weekly intervals after delayed post-SCI administration of SWNTs (gray bars, days 14–35 post-injury). SCI induced an acute reduction in latency in all conditions (pre-injury values versus post-SCI values on day 5, indicated by \*). However, no significant differences in tail-flick latency were observed between post-injury day 5 values (before administration of SWNT), and post-injury day 14–35 values for any treatment group. Also, no significant differences between post-injury day 14 (after SWNT administration) and post-injury day 21–35 values were found for any treatment group (SCI, spinal cord injury; SWNT-PEG, single-walled carbon nanotubes functionalized with polyethylene glycol).

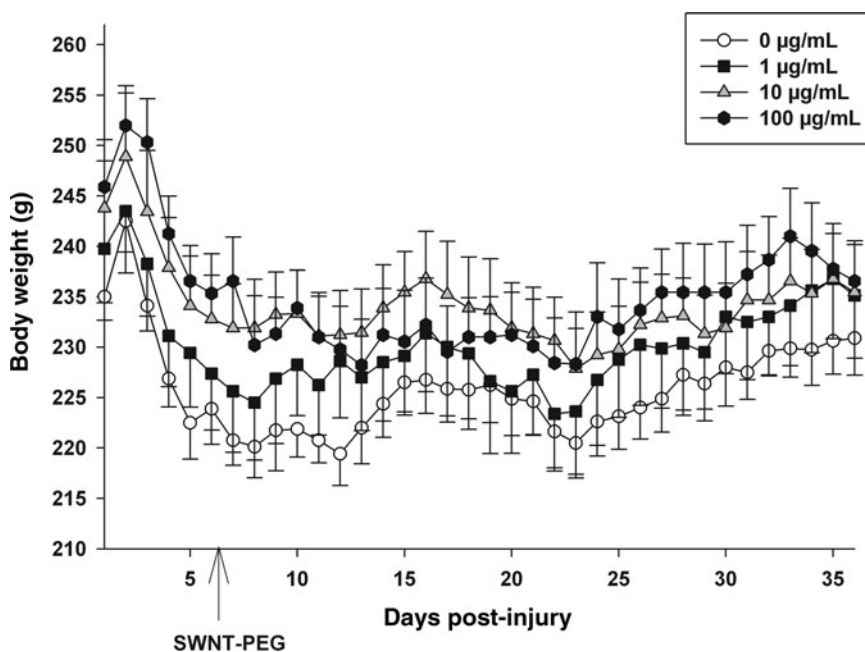


**FIG. 9.** Effect of delayed post-SCI administration of SWNT-PEG on daily body weight. The animals were inspected daily and the body weight (in grams) recorded as an indicator of overall health. SCI induced a loss of average body weight in all treatment groups. No significant differences were found between the average body weights recorded on post-SCI day 5 (before SWNT-PEG administration) and post-SCI days 8–35 (after SWNT-PEG administration) for any treatment group evaluated. SWNT-PEG administration is indicated by the arrow (post-SCI day 7; SCI, spinal cord injury; SWNT-PEG, single-walled carbon nanotubes functionalized with polyethylene glycol).

Also, Hejcl and colleagues demonstrated that hydrogel (based on 2-hydroxypropylmethacrylamide) seeded with mesenchymal stem cells induces functional recovery after SCI in adult rats (Hejcl et al., 2010). It has recently been shown that the scale of the scaffold alters the extent of tissue repair and regenerating axons in the transected spinal cord, with smaller-scale scaffolds imparting greater improvement (Krych et al., 2009).

Nanometer-scale materials, more specifically nanofibers, may potentially afford increased biocompatibility, as the small diameter more closely mimics the scale of CNS tissue. Additionally, nanomaterials can be manipulated to enhance the growth-promoting properties (Malarkey and Parpura, 2007; Sucupane et al., 2009), that when appropriately developed into regenerative scaffolds may obviate the need for controversial and risky stem cell-based or tissue extract-based components. Furthermore, since carbon nanotubes (CNTs) are not biodegradable they can influence the recovery of injured tissue for a prolonged period of time. We report in this study that application of SWNT-PEG did not induce reactive gliosis, which is similar to a previous finding that peptide amphiphile nanofibers did not induce glial scar formation in a mouse model of SCI (Tysseling-Mattiace et al., 2008). Furthermore, we demonstrated in this study that delayed post-SCI administration of SWNT-PEG induced tissue repair, axonal repair/regeneration, and functional recovery. However, the functional recovery and repair/regeneration in the CST were both modest. An important caveat in the interpretation of these data is that we utilized a complete transection injury model that induces a sizeable lesion in the rat spinal cord. The advantage to this SCI model is that all descending and ascending tracts are severed, thereby eliminating (or substantially reducing) the contribution of uninjured (spared) tissue to functional recovery (Steward et al., 2003). On the other hand, substantial regeneration/repair are much more difficult to achieve in a complete transection model than in models with more limited injury. Although we observed modest functional recovery using SWNT-PEG, this material could be further improved to promote regeneration and regrowth. Strategies for improving the growth-promoting characteristics of SWNTs could include functionalization with growth factors, as it is well-established that administration of neurotrophins (NTs), in particular nerve growth factor (NGF), neurotrophin-3, or brain-derived neurotrophic factor (BDNF), to the injured spinal cord promotes axonal outgrowth and regeneration (Blesch and Tuszynski, 2002). Proof of concept of functionalization of nanotubes with growth factors has been demonstrated by Matsumoto and colleagues (Matsumoto et al., 2007), who covalently linked NGF or BDNF to MWNTs, and demonstrated improved dorsal root ganglia neurite outgrowth.

An additional characteristic of SWNTs that may be harnessed to promote repair and recovery of neuronal circuitry after SCI is the conductive properties of carbon nanotubes (Lee and Parpura, 2009). It has previously been shown that primary neuronal cultures grown on carbon nanotube substrates demonstrate enhanced electrical activity (Lovat et al., 2005; Mazzatenta et al., 2007). Also, Cellot and colleagues (Cellot et al., 2009) recently found that carbon nanotubes can function as an electrical shortcut between somatic and dendritic neuronal compartments, which results in enhanced neuronal excitability. Similarly, we (Malarkey et al., 2009)

systematically varied the conductivity of scaffolds made of SWNT films and evaluated the effects on neurite outgrowth *in vitro*. SWNT films with a certain conductance promoted increased outgrowth of neurites and increased cell body area. Thus, taken together, these studies indicate that the nanoscale material substrate may be useful for enhancing neuronal signaling by direct contact with neurons, and that the conductive properties of the CNTs can be manipulated to optimize neuronal repair/regrowth, making this material an intriguing substrate for use as scaffolding after SCI.

Another potential mechanism of the tissue repair that we found with SWNT-PEG administration could be the effects of PEG on resealing damaged cellular membranes, as previous work in animal and tissue culture models of SCI has demonstrated protective effects of PEG (Shi and Borgens, 1999, 2000; Shi et al., 1999). For example, Baptiste and colleagues reported that post-SCI administration of PEG reduces injury-induced tissue cavitation and increases tissue preservation, reduces neurofilament degradation, and enhances axonal integrity. However, only modest functional recovery was observed (Baptiste et al., 2009). Similarly, Ditor and colleagues (Ditor et al., 2007) evaluated the effect of post-SCI administration of PEG alone or in combination with MgSO<sub>4</sub> in a rat model, and reported that PEG administration reduced at-level neuropathic pain and modestly improved hindlimb locomotor function, which was associated with decreases in lesion volume. More recently it has been demonstrated that PEG-decorated silica nanoparticles sealed damaged cell membranes and improved axonal function after SCI (Cho et al., 2010). Taken collectively, our data are consistent with this previous literature that demonstrates the reparative properties of PEG after SCI. Indeed, since we have previously shown that soluble SWNTs grafted by either PEG or poly-*m*-aminobenzenesulfonic acid (PABS) enhance the outgrowth of selected neurites (Ni et al., 2005) by blocking stimulated endocytosis (Malarkey et al., 2009), we selected the grafted copolymer SWNT-PEG in an attempt to combine PEG's effect of resealing the plasma membrane with SWNT's ability to modulate neurite outgrowth in SCI. An important issue to consider is that SWNT-PEG administration would not be expected to result in detectable levels of free PEG due to the covalent bond. Additionally, in the current study we did not directly compare the effects of SWNT-PEG to injection of PEG alone. Thus it remains an open question if PEG chemically bound to SWNTs can function in resealing plasma membranes as has been demonstrated for the free form of PEG.

In conclusion, we report here that post-SCI administration of SWNT-PEG, especially at a concentration of 100  $\mu\text{g}/\text{mL}$ , improves axonal repair and regeneration into the lesion cavity and induces modest functional recovery, which suggests that this may be an effective nanomaterial to apply for promoting recovery after SCI. Future studies will explore the use of SWNTs functionalized with growth factors, as well as the evaluation of charged SWNTs, as strategies to further promote repair and regeneration of damaged spinal cord tissue.

#### Acknowledgments

We thank Dr. Bin Zhao (University of California, Riverside) for functionalization of SWNTs. This study was supported by the UAB BioMatrix Engineering and Regenerative Medicine (BERM) Center Pilot Grant (C.L.F. and V.P.), the Center for

Glial Biology in Medicine, and the Department of Physical Medicine and Rehabilitation. This study was also supported by the Ronald E. McNair Post-Baccalaureate Achievement Program (J.A.R.), the Wachovia Scholars Foundation Fund (J.A.R.), and by grants from the National Institute of Mental Health (R01 MH 069791 to V.P.), and the National Science Foundation (CBET 0943343 to V.P.). The stereology microscope was provided by a National Institutes of Health Neuroscience Blueprint Core Grant to the University of Alabama at Birmingham (NS57098).

#### Author Disclosure Statement

No competing financial interests exist.

#### References

- Anderson, D.K., and Hall, E.D. (1993). Pathophysiology of spinal cord trauma. *Ann. Emerg. Med.* 22, 987–992.
- Anderson, D.K., Howland, D.R., and Reier, P.J. (1995). Fetal neural grafts and repair of the injured spinal cord. *Brain Pathol.* 5, 451–457.
- Baptiste, D.C., Austin, J.W., Zhao, W., Nahirny, A., Sugita, S., and Fehlings, M.G. (2009). Systemic polyethylene glycol promotes neurological recovery and tissue sparing in rats after cervical spinal cord injury. *J. Neuropathol. Exp. Neurol.* 68, 661–676.
- Basso, D.M., Beattie, M.S., and Bresnahan, J.C. (1995). A sensitive and reliable locomotor rating scale for open field testing in rats. *J. Neurotrauma* 12, 1–21.
- Bekyarov, E., Ni, Y., Malarkey, E.B., Montana, V., McWilliams, J.L., Haddon, R.C., and Parpura, V. (2005). Applications of carbon nanotubes in biotechnology and biomedicine. *J. Biomed. Nanotechnol.* 1, 3–17.
- Blesch, A., and Tuszynski, M.H. (2002). Spontaneous and neurotrophin-induced axonal plasticity after spinal cord injury. *Prog. Brain Res.* 137, 415–423.
- Bunge, M.B., and Pearse, D.D. (2003). Transplantation strategies to promote repair of the injured spinal cord. *J. Rehabil. Res. Dev.* 40, 55–62.
- Calancie, B., Madsen, P.W., Wood, P., Marcillo, A.E., Levi, A.D., and Bunge, R.P. (2009). A guidance channel seeded with autologous Schwann cells for repair of cauda equina injury in a primate model. *J. Spinal Cord. Med.* 32, 379–388.
- Cellot, G., Cilia, E., Cipollone, S., Rancic, V., Sucapane, A., Giordani, S., Gambazzi, L., Markram, H., Grandolfo, M., Scaini, D., Gelain, F., Casalis, L., Prato, M., Giugliano, M., and Ballerini, L. (2009). Carbon nanotubes might improve neuronal performance by favouring electrical shortcuts. *Nat. Nanotechnol.* 4, 126–133.
- Chaovipoch, P., Jelks, K.A., Gerhold, L.M., West, E.J., Chongthammakun, S., and Floyd, C.L. (2006). 17beta-estradiol is protective in spinal cord injury in post- and pre-menopausal rats. *J. Neurotrauma* 23, 830–852.
- Chaplan, S.R., Bach, F.W., Pogrel, J.W., Chung, J.M., and Yaksh, T.L. (1994). Quantitative assessment of tactile allodynia in the rat paw. *J. Neurosci. Methods* 53, 55–63.
- Cheng, H., Cao, Y., and Olson, L. (1996). Spinal cord repair in adult paraplegic rats: partial restoration of hind limb function. *Science* 273, 510–513.
- Cho, Y., Shi, R., Ivanisevic, A., and Borgens, R.B. (2010). Functional silica nanoparticle-mediated neuronal membrane sealing following traumatic spinal cord injury. *J. Neurosci. Res.* 88, 1433–1444.
- Deakin, J.F., and Dostrovsky, J.O. (1978). Involvement of the periaqueductal grey matter and spinal 5-hydroxytryptaminergic pathways in morphine analgesia: effects of lesions and 5-hydroxytryptamine depletion. *Br. J. Pharmacol.* 63, 159–165.
- Ditor, D.S., John, S.M., Roy, J., Marx, J.C., Kittner, C., and Weaver, L.C. (2007). Effects of polyethylene glycol and magnesium sulfate administration on clinically relevant neurological outcomes after spinal cord injury in the rat. *J. Neurosci. Res.* 85, 1458–1467.
- Hamers, F.P., Koopmans, G.C., and Joosten, E.A. (2006). CatWalk-assisted gait analysis in the assessment of spinal cord injury. *J. Neurotrauma* 23, 537–548.
- Hejcl, A., Sedy, J., Kapcalova, M., Arboleda, T.D., Amemori, T., Likavcanova-Masinova, K., Lesny, P., Krumbholcova, E., Pradny, M., Michalek, J., Burian, M., Hajek, M., Jendelova, P., and Sykova, E. (2010). HPMA-RGD hydrogels seeded with mesenchymal stem cells improve functional outcome in chronic spinal cord injury. *Stem Cells Dev.* [Epub ahead of print].
- Hu, H., Ni, Y., Montana, V., Haddon, R.C., and Parpura, V. (2004). Chemically functionalized carbon nanotubes as substrates for neuronal growth. *Nano Letters* 4, 507–511.
- Hu, H., Ni, Y., Swadhin, K.M., Montana, V., Zhao, B., Haddon, R.C., and Parpura, V. (2005). Polyethyleneimine functionalized single-walled carbon nanotubes as a substrate for neuronal growth. *J. Phys. Chem. Lett.* 109, 4285–4289.
- Johnson, P.J., Parker, S.R., and Sakiyama-Elbert, S.E. (2010a). Fibrin-based tissue engineering scaffolds enhance neural fiber sprouting and delay the accumulation of reactive astrocytes at the lesion in a subacute model of spinal cord injury. *J. Biomed. Mater. Res. A* 92, 152–163.
- Johnson, P.J., Tataru, A., Shiu, A., and Sakiyama-Elbert, S.E. (2010b). Controlled release of neurotrophin-3 and platelet-derived growth factor from fibrin scaffolds containing neural progenitor cells enhances survival and differentiation into neurons in a subacute model of SCI. *Cell Transplant* 19, 89–101.
- Kachadroka, S., Hall, A.M., Niedzielko, T.L., Chongthammakun, S., and Floyd, C.L. (2010). Effect of endogenous androgens on 17beta-estradiol-mediated protection after spinal cord injury in male rats. *J. Neurotrauma* 27, 611–626.
- Krych, A.J., Rooney, G.E., Chen, B., Schermerhorn, T.C., Ameenuddin, S., Gross, L., Moore, M.J., Currier, B.L., Spinner, R.J., Friedman, J.A., Yaszemski, M.J., and Windebank, A.J. (2009). Relationship between scaffold channel diameter and number of regenerating axons in the transected rat spinal cord. *Acta Biomater.* 5, 2551–2559.
- Kuhlengel, K.R., Bunge, M.B., and Bunge, R.P. (1990a). Implantation of cultured sensory neurons and Schwann cells into lesioned neonatal rat spinal cord. I. Methods for preparing implants from dissociated cells. *J. Comp. Neurol.* 293, 63–73.
- Kuhlengel, K.R., Bunge, M.B., Bunge, R.P., and Burton, H. (1990b). Implantation of cultured sensory neurons and Schwann cells into lesioned neonatal rat spinal cord. II. Implant characteristics and examination of corticospinal tract growth. *J. Comp. Neurol.* 293, 74–91.
- Lee, W., and Parpura, V. (2009). Wiring neurons with carbon nanotubes. *Front. Neuroengineering* 2, 8.
- Lovat, V., Pantarotto, D., Lagostena, L., Cacciari, B., Grandolfo, M., Righi, M., Spalluto, G., Prato, M., and Ballerini, L. (2005). Carbon nanotube substrates boost neuronal electrical signaling. *Nano Lett.* 5, 1107–1110.
- Malarkey, E.B., and Parpura, V. (2007). Applications of carbon nanotubes in neurobiology. *Neurodegener. Dis.* 4, 292–299.

- Malarkey, E.B., Fisher, K.A., Bekyarova, E., Liu, W., Haddon, R.C., and Parpura, V. (2009). Conductive single-walled carbon nanotube substrates modulate neuronal growth. *Nano Lett.* 9, 264–268.
- Malarkey, E.B., Reyes, R.C., Zhao, B., Haddon, R.C., and Parpura, V. (2008). Water soluble single-walled carbon nanotubes inhibit stimulated endocytosis in neurons. *Nano Lett.* 8, 3538–3542.
- Matsumoto, K., Sato, C., Naka, Y., Kitazawa, A., Whitby, R.L., and Shimizu, N. (2007). Neurite outgrowths of neurons with neurotrophin-coated carbon nanotubes. *J. Bioscience Bioengineering* 103, 216–220.
- Mazzatenta, A., Giugliano, M., Campidelli, S., Gambazzi, L., Businaro, L., Markram, H., Prato, M., and Ballerini, L. (2007). Interfacing neurons with carbon nanotubes: electrical signal transfer and synaptic stimulation in cultured brain circuits. *J. Neurosci.* 27, 6931–6936.
- McDonald, J.W., Liu, X.Z., Qu, Y., Liu, S., Mickey, S.K., Turetsky, D., Gottlieb, D.I., and Choi, D.W. (1999). Transplanted embryonic stem cells survive, differentiate and promote recovery in injured rat spinal cord. *Nat. Med.* 5, 1410–1412.
- National Spinal Cord Injury Statistical Center. (2008). Spinal cord injury information network. <http://www.spinalcord.uab.edu/>
- Ni, Y., Hu, H., Malarkey, E.B., Zhao, B., Montana, V., Haddon, R.C., and Parpura, V. (2005). Chemically functionalized water soluble single-walled carbon nanotubes modulate neurite outgrowth. *J. Nanosci. Nanotechnol.* 5, 1707–1712.
- Norenberg, M.D., Smith, J., and Marcillo, A. (2004). The pathology of human spinal cord injury: defining the problems. *J. Neurotrauma* 21, 429–440.
- Novikova, L.N., Novikov, L.N., and Kellerth, J.O. (2003). Biopolymers and biodegradable smart implants for tissue regeneration after spinal cord injury. *Curr. Opin. Neurol.* 16, 711–715.
- Oudega, M., Gautier, S.E., Chapon, P., Fragoso, M., Bates, M.L., Parel, J.M., and Bunge, M.B. (2001). Axonal regeneration into Schwann cell grafts within resorbable poly(alpha-hydroxyacid) guidance channels in the adult rat spinal cord. *Biomaterials* 22, 1125–1136.
- Park, J., Lim, E., Back, S., Na, H., Park, Y., and Sun, K. (2010). Nerve regeneration following spinal cord injury using matrix metalloproteinase-sensitive, hyaluronic acid-based biomimetic hydrogel scaffold containing brain-derived neurotrophic factor. *J. Biomed. Mater. Res. A* 93, 1091–1099.
- Park, K.I., Liu, S., Flax, J.D., Nissim, S., Stieg, P.E., and Snyder, E.Y. (1999). Transplantation of neural progenitor and stem cells: developmental insights may suggest new therapies for spinal cord and other CNS dysfunction. *J. Neurotrauma* 16, 675–687.
- Potter, W., Kalil, R.E., and Kao, W.J. (2008). Biomimetic material systems for neural progenitor cell-based therapy. *Front. Biosci.* 13, 806–821.
- Raju, D.V., and Smith, Y. (2006). Anterograde axonal tract tracing. *Curr. Protoc. Neurosci.* Chapter 1.
- Ramon-Cueto, A., Plant, G.W., Avila, J., and Bunge, M.B. (1998). Long-distance axonal regeneration in the transected adult rat spinal cord is promoted by olfactory ensheathing glia transplants. *J. Neurosci.* 18, 3803–3815.
- Reiner, A., Veenman, C.L., Medina, L., Jiao, Y., Del, M.N., and Honig, M.G. (2000). Pathway tracing using biotinylated dextran amines. *J. Neurosci. Methods* 103, 23–37.
- Shi, R., and Borgens, R.B. (1999). Acute repair of crushed guinea pig spinal cord by polyethylene glycol. *J. Neurophysiol.* 81, 2406–2414.
- Shi, R., and Borgens, R.B. (2000). Anatomical repair of nerve membranes in crushed mammalian spinal cord with polyethylene glycol. *J. Neurocytol.* 29, 633–643.
- Shi, R., Borgens, R.B., and Blight, A.R. (1999). Functional reconnection of severed mammalian spinal cord axons with polyethylene glycol. *J. Neurotrauma* 16, 727–738.
- Steward, O., Zheng, B., and Tessier-Lavigne, M. (2003). False resurrections: distinguishing regenerated from spared axons in the injured central nervous system. *J. Comp. Neurol.* 459, 1–8.
- Sucapane, A., Cellot, G., Prato, M., Giugliano, M., Parpura, V., and Ballerini, L. (2009). Interactions between cultured neurons and carbon nanotubes: A nanoneuroscience vignette. *J. Nanoneurosci.* 1, 10–16.
- Tabesh, H., Amoabediny, G., Nik, N.S., Heydari, M., Yosefifard, M., Siadat, S.O., and Mottaghy, K. (2009). The role of biodegradable engineered scaffolds seeded with Schwann cells for spinal cord regeneration. *Neurochem. Int.* 54, 73–83.
- Tysseling-Mattiace, V.M., Sahni, V., Niece, K.L., Birch, D., Czeisler, C., Fehlings, M.G., Stupp, S.I., and Kessler, J.A. (2008). Self-assembling nanofibers inhibit glial scar formation and promote axon elongation after spinal cord injury. *J. Neurosci.* 28, 3814–3823.
- Wang, Y., Lapitsky, Y., Kang, C.E., and Shoichet, M.S. (2009). Accelerated release of a sparingly soluble drug from an injectable hyaluronan-methylcellulose hydrogel. *J. Control Release* 140, 218–223.
- West, M.J., Slomianka, L., and Gundersen, H.J. (1991). Unbiased stereological estimation of the total number of neurons in the subdivisions of the rat hippocampus using the optical fractionator. *Anat. Rec.* 231, 482–497.
- Wouterlood, F.G., Goede, P.H., and Groenewegen, H.J. (1990). The in situ detectability of the neuroanatomical tracer *Phaseolus vulgaris*-leucoagglutinin (PHA-L). *J. Chem. Neuroanat.* 3, 11–18.
- Xu, X.M., Guenard, V., Kleitman, N., and Bunge, M.B. (1995). Axonal regeneration into Schwann cell-seeded guidance channels grafted into transected adult rat spinal cord. *J. Comp. Neurol.* 351, 145–160.

Address correspondence to:

Candace L. Floyd, Ph.D.

Department of Physical Medicine and Rehabilitation

Center for Glial Biology in Medicine

University of Alabama, Birmingham

546 Spain Rehabilitation Center

1717 Sixth Avenue South

Birmingham, AL 35249

E-mail: clfloyd@uab.edu